AGU ADVANCING EARTH AND SPACE SCIENCE

Geophysical Research Letters

RESEARCH LETTER
10.1029/2021GL092950

Key Points:

- The frictional properties of the Whillans Ice Stream bed are spatially heterogeneous
- Seismic velocities are sensitive to small changes in till poroelastic properties
- Dilatant strengthening of till stabilizes the glacier during stick-slip cycles

Supporting Information:

Supporting Information may be found in the online version of this article.

Correspondence to:

A. Mordret,
aurelien.mordret@univ-grenoble-alpes.fr

Citation:

Guerin, G., Mordret, A., Rivet, D., Lipovsky, B. P., & Minchew, B. M. (2021). Frictional origin of slip events of the Whillans Ice Stream, Antarctica. *Geophysical Research Letters*, *48*, e2021GL092950. https://doi.org/10.1029/2021GL092950

Received 11 FEB 2021
Accepted 13 MAY 2021

Author Contributions:

Conceptualization: Aurélien Mordret
Formal analysis: Gauthier Guerin, Aurélien Mordret, Diane Rivet
Funding acquisition: Aurélien Mordret, Diane Rivet
Investigation: Gauthier Guerin, Aurélien Mordret, Diane Rivet
Methodology: Aurélien Mordret
Resources: Brent M. Minchew
Software: Gauthier Guerin, Aurélien Mordret, Diane Rivet
Supervision: Aurélien Mordret, Diane Rivet, Brent M. Minchew
Validation: Gauthier Guerin, Aurélien Mordret, Diane Rivet, Bradley P. Lipovsky, Brent M. Minchew
Visualization: Gauthier Guerin, Aurélien Mordret
Writing – original draft: Gauthier Guerin
Writing – review & editing: Aurélien Mordret, Diane Rivet, Bradley P. Lipovsky, Brent M. Minchew

Frictional Origin of Slip Events of the Whillans Ice Stream, Antarctica

Gauthier Guerin[1], Aurélien Mordret[2,3], Diane Rivet[1], Bradley P. Lipovsky[4], and Brent M. Minchew[3]

[1]Université Côte d'Azur, CNRS, Observatoire de la Côte d'Azur, IRD, Géoazur, Valbonne, France, [2]Université Grenoble Alpes, Univ. Savoie Mont Blanc, CNRS, IRD, IFSTTAR, ISTerre, Grenoble, France, [3]Department of Earth, Atmospheric and Planetary Sciences, Massachusetts Institute of Technology (MIT), Cambridge, MA, USA, [4]Department of Earth and Planetary Sciences, Harvard University, Cambridge, MA, USA

Abstract Ice sheet evolution depends on subglacial conditions, with the ice-bed interface's strength exerting an outsized role on the ice dynamics. Along fast-flowing glaciers, this strength is often controlled by the deformation of subglacial till, making quantification of spatial variations of till strength essential for understanding ice-sheet contribution to sea-level. This task remains challenging due to a lack of in situ observations. We analyze continuous seismic data from the Whillans Ice Plain (WIP), West Antarctica, to uncover spatio-temporal patterns in subglacial conditions. We exploit tidally modulated stick-slip events as a natural source of sliding variability. We observe a significant reduction of the till seismic wave-speed between the WIP sticky-spots. These observations are consistent with a poroelastic model where the bed experiences relative porosity and effective pressure increases of >11% during stick-slips. We conclude that dilatant strengthening appears to be an essential mechanism in stabilizing the rapid motion of fast-flowing ice streams.

Plain Language Summary The rate of ice-mass loss from the Antarctic ice-sheet, and hence sea-level rise, is governed by the rate of ice flow. The frictional force of the glacier bed plays a large role in ice flow speed. For fast glaciers, this force is often controlled by the deformation of subglacial sediments. Therefore, understanding their mechanical properties is crucial to understanding glaciers' contribution to sea-level rise. This task remains challenging due to the lack of direct, in-situ observations. This paper analyzes seismic data recorded on the Whillans Ice Plain (WIP) in West Antarctica to reveal spatio-temporal phenomena in subglacial conditions. We exploit glacier stick-slip events as natural sources of slip variability. We observe a significant reduction in seismic wave-speed within the till between the WIP's sticky-spots. On the contrary, the sticky-spots themselves show no change. These observations are consistent with a poroelastic model. In between the sticky-spots, the bed undergoes an increase in effective pressure and porosity due to the sediments' plowing during the slip. These till variations slow down the glacier slip and prevent it from accelerating catastrophically. This phenomenon of strengthening by dilation of bed sediments appears to be an essential mechanism for stabilizing the rapid movement of fast-flowing ice-streams.

1. Introduction

Sea level rise (SLR) is among the most significant long-term consequences of global warming with direct economic, societal, and cultural impacts (Nicholls & Cazenave, 2010). Given the enormous volume of ice sitting in low-elevation basins located below sea level, the Antarctic ice sheet has the potential to become the largest contributor to future SLR. This contribution, however, remains highly uncertain (Alley et al., 2005; Golledge et al., 2019; Oppenheimer, 1998; Pachauri et al., 2014). The single largest source of this uncertainty in most simulations of long-term ice flow is the representation of glacier sliding physics (Cornford et al., 2020). Glacier sliding physics is most often understood through idealized theoretical models (Meyer et al., 2018; Schoof, 2005; Weertman, 1964) and laboratory experiments (Iverson et al., 2003; Tulaczyk et al., 2000; Wu et al., 2008; Zoet & Iverson, 2020). Although these are both important lines of investigation, both theoretical and laboratory results must be validated against field observations to confirm that they capture the correct physical processes.

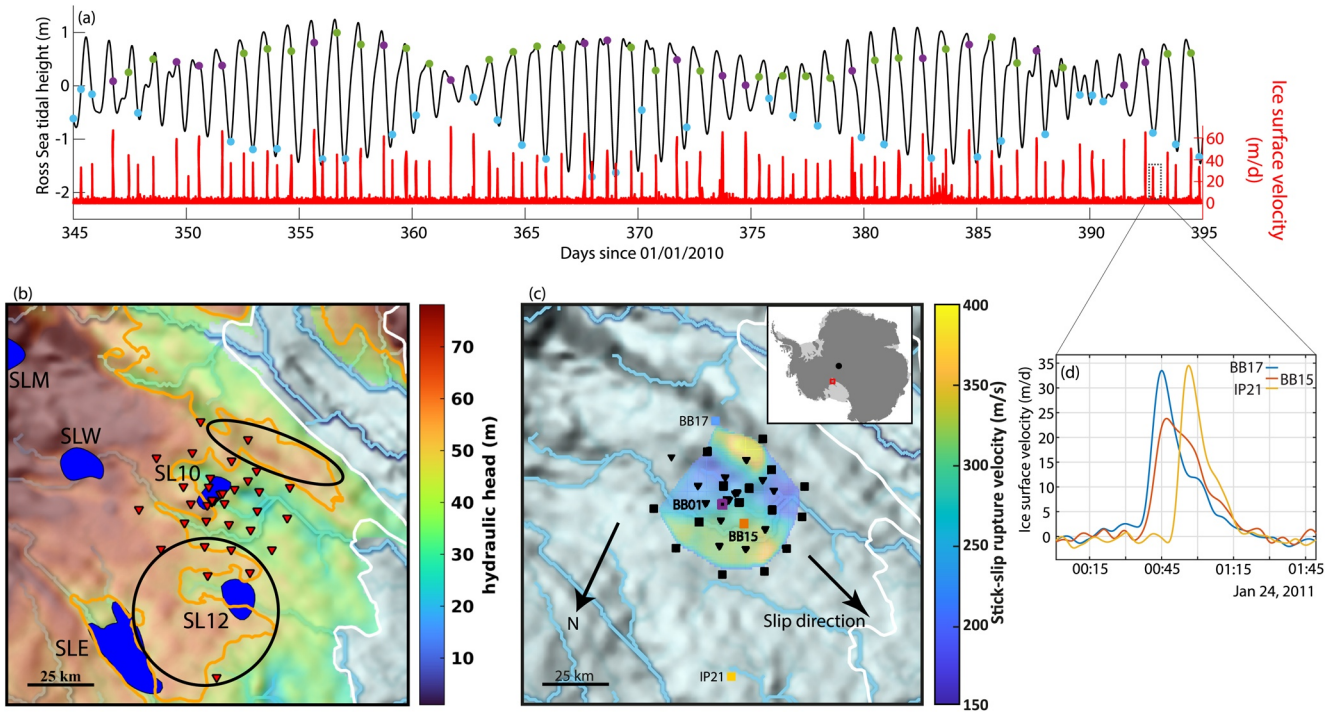

Figure 1. The Whillans Ice Plain data set. (a) Ross Sea tidal height (black curve). The dots are the origin-time of the stick-slip event: Blue for low tides, green for high tides, and purple for events after a low-tide skipped event. The red curve represents the ice surface velocity recorded at GPS BB01 (purple square in c) during the studied period. (b) Contextual map of the studied area with the seismic network shown with the red triangles. The shaded background is the bed topography from Bedmap2 (Fretwell et al., 2013) overlaid by the hydraulic head (in color). The thick orange curve is the 50 m hydraulic head level highlighting the lateral heterogeneity of the bed across the WIP. The black ellipses show the locations of the sticky spots. The blue patches are the subglacial lakes: Subglacial Lake Mercer (SLM), Subglacial Lake Whillans (SLW) and Subglacial Lake Engelhardt (SLE) (Siegfried & Fricker, 2018). The light blue lines in (b) and (c) are subglacial water flow paths based on hydropotential gradients (Siegfried & Fricker, 2018) showing the bottom of valleys. The white curve is the grounding line estimated by InSAR (Mouginot et al., 2016). (c) Map of the stick-slip rupture velocity. Seismic stations (black triangle) and co-located GPS and seismic stations (black square) are displayed. The background shows the bed topography as in (b). (d) GPS signals from BB17 (blue), BB15 (red), and IP21 (yellow) stations, indicated in (c), recorded during a single stick-slip cycle.

Direct borehole access to the bed has demonstrated the importance of high water pressure and subglacial till in facilitating fast sliding in the Antarctic ice streams (Alley et al., 1986; Kamb, 2001). Borehole access, however, is limited to point measurements in space. At the scale of a glacier or ice stream, geophysical measurements–with their ability to cover large areas–are needed to understand variability in basal boundary conditions (Bamber et al., 2001; Blankenship et al., 1986; Brisbourne et al., 2017; Luthra et al., 2016; Tulaczyk et al., 2000). Nevertheless, due to logistical constraints, geophysical campaigns are mostly performed at a fixed point in time, and therefore provide a static snapshot of the bed conditions and structure. Here, we reprocessed seismic and geodetic data from a past experiment (Winberry et al., 2013) to characterize the in-situ mechanical properties of glacial till beneath the Whillans Ice Plain (WIP), West Antarctica (Figure 1), both in time and space. We show that the spatio-temporal mechanical properties of the bed control the unique short-term sliding behavior of the ice stream. Our experimental design hinges on the unique sliding behavior of the WIP.

2. Whillans Ice Plain Stick-Slip Cycles

The WIP is a 120 km wide and 700 m thick outlet glacier in the northern part of the Whillans Ice Stream in West Antarctica. WIP rests on a 6–10 m thick basal till layer (Luthra et al., 2016) and is unique in its displacement as it advances into the Ross Ice Shelf through predictable large-scale stick-slip cycles (Bindschadler et al., 2003; Winberry et al., 2009) that are triggered twice a day by the ocean tides (Figure 1a). Over the past decades, WIP has decelerated (Joughin et al., 2005), possibly due to the feedback between ice flow,

frictional heating, and the hydromechanical properties of the subglacial till, namely dilation and pore water pressure (Tulaczyk et al., 2000).

The stick-slip motions of WIP are controlled by regions of high basal friction (asperities or "sticky spots" (Alley, 1993; Stokes et al., 2007)) at the ice/till interface (Winberry et al., 2011). These sticky spots are located at the far north and south of the ice stream and correspond to high hydraulic potentials caused by a valley-like bed topography underneath the ice (Figure 1b), with its lowest points in the central part of the stream (Winberry et al., 2014). During a stick-slip cycle, the glacier is locked on the sticky spots, then when the tides favorably modulate the basal friction on the terminus of the glacier, usually just after high tide and at low tide (Lipovsky & Dunham, 2017; Robel et al., 2017; Minchew et al., 2017), the glacier starts accelerating from one sticky spot with a surface velocity about 40 m/d for about 45 min (Figures 1a–1c). The slip is slowed down by about 30% in the central section of the stream, and then it accelerates again on the second sticky spot (Figure 1c). Since not all parts of the glacier start moving at once, the surface motion gradient generates a rupture front-like propagation crossing the WIP perpendicular to its general direction of motion (Lipovsky & Dunham, 2017). Analysis of GPS data at the surface (Figure 1b, see Supporting Information Text S1 for a detailed description of the estimation of the rupture velocity from the GPS data) shows that the velocity of the rupture of the glacier-bed interface varies laterally, from fast-slip at about 400 m/s on the sticky spots to slow-slip at less than 200 m/s in between the sticky spots, corresponding to the deepest part of the sub-glacial valley.

The exact nature of the sticky spots is still debated, but modeling (Lipovsky & Dunham, 2017; Lipovsky et al., 2019) and seismological observations (Barcheck et al., 2018, 2020; Lipovsky & Dunham, 2016; Pratt et al., 2014; Wiens et al., 2008) have revealed that the sticky spots are seismogenic while the areas between them are not. This seismic/aseismic behavior implies lateral variations in the frictional properties of the till layer across the WIP, with sticky spots corresponding to zones of rate-weakening friction and the rest of the ice stream consisting of rate-strengthening regions (Lipovsky & Dunham, 2017).

Here we use the stick-slip motion of the glacier as a transient perturbation to probe its effects on the subglacial system. The perturbation is monitored using ambient seismic noise correlations (Brenguier et al., 2014) thanks to the high sensitivity of seismic waves to the poroelastic properties of the bed, as well as their temporal changes (Mordret et al., 2016). Analyzing the seismic velocities during stick-slip cycles, we highlight the lateral heterogeneity in these properties responsible for the slow-slip motion in the central area of the WIP.

3. Seismic Velocity Changes During Slip Events

We use time series from 22 GPS and 33 broadband seismic stations installed on WIP during 50 days of the 2010–2011 austral summer field season (Figure 1b). During this period, the geodetic and seismic networks simultaneously recorded 78 stick-slip cycles. To obtain a sufficient temporal resolution to observe seismic velocity changes during a stick-slip cycle, we use the four correlation components containing Rayleigh waves and we stack the cross-correlations relative to the time onset of every 78 cycles (Figure S1, see Supporting Information Text S2 for details of the seismic data processing), a scheme inspired by the approach of Hillers et al. (2015). In doing so, we assume that the ice and bed deform during the stick phases and rebound during the slip phases by similar amounts, and that the displacement of the ice during slip is comparable. The minimum inter-event duration is eight hours, thus we chose an eight-hour window centered on each stick-slip event to observe the steady state before the event without being disturbed by the end of the previous event. After the events, the medium recovers to a steady state over a period of around four hours. We achieve a 5-min temporal resolution by correlating 10-min long segments of seismic noise with 50% overlap between segments and by post-processing the correlations for a single station-pair with a Wiener filter (Moreau et al., 2017). Effectively, each correlation is a stack of 13 h of seismic signals, allowing a ten-fold increase of the signal-to-noise ratio, and therefore in the precision of the measurement of the velocity changes (Silver et al., 2007). We performed the analysis on two subsets of the correlations built from the stack of the low-tide events only and the high-tide events only. The result of stacking twice less data clearly decreases the quality of the correlations. The resulting velocity change curves show similar patterns for both subsets which are also similar to the overall stack over the 78 events (see below), but are much more noisy.

This renders the interpretation of any difference between the low-tide and high-tide events difficult. Ideally, we would like to be able to analyze individual events independently, but this goal would probably require a different data set from a denser seismic array.

We measured the relative Rayleigh-wave velocity changes (dc/c) in the [0.2–0.5] Hz frequency band in the early coda of the correlations (Brenguier et al., 2014). We chose this frequency band because it provides high-enough frequencies to probe the first hundred meters of the subsurface, being sensitive to both the glacier and its bed. The seismic energy is larger in the lower half of this frequency band and therefore we expect that the overall sensitivity of our dc/c measurements are dominated by the low frequency side (Figure S2). Only very short inter-station distance correlations exhibit significant energy above 0.5 Hz. Measurements in narrower frequency bands within the [0.2–0.5] Hz frequency band provide similar results albeit more unstable and noisier. Using a linear inversion of the dc/c measurements from all possible pairs of 10-min correlations, we obtained 528 eight-hour-long time series of relative seismic velocity changes, one for each pair of seismic stations (see Supporting Information Text S3 for more details on the processing). The global average of dc/c (Figure 2i) shows a significant reduction of the seismic velocity ($\sim$0.04% $\pm$ 0.005%) starting at the end of the slipping period (Figure 2). The exact onset of the velocity decrease is unclear due to the measurement uncertainties. It could be either at $t = 0$ of the events or about 40 min before, hinting to a possible precursory phase of the rupture (Barcheck et al., 2021; Winberry et al., 2013). It is worth noting that the velocity drops during the pre-slip phase and during the main slip phase seem to scale with the displacement during each phase (the pre-slip phase representing 1/4 of the total displacement and 1/4 of the total velocity drop; Barcheck et al. (2021)). During the four hours after the slip, the velocity increases back to the pre-slip level. Oscillations with $\sim$75 min period and amplitude of about 0.02% seem to overlay the velocity recovery. This oscillation could be due to a resonance of the whole WIP generated by the excitation of the stick-slip events. For instance, this period matches quite well with the fundamental eigenmode period of a free-standing $\sim 100 \times 100$ km^2 plate of ice of 800 m thickness, which is equal to $\sim$73 min (Text S4, Jones (1975)). We are not aware of similar observations in other contexts such as tectonic faults or laboratory experiments, which could corroborate this thin-plate geometry interpretation rather unique to glacier environments. During the four hours preceding the slip, the steady velocity increase is probably due to the effect of the preceding stick-slip cycles or a signature of the constant loading from the upstream glacier.

By averaging the dc/c time series sharing a common station (Brenguier et al., 2014), we obtain 33 average dc/c curves that we associate with the location of each station (Hobiger et al., 2012; Obermann et al., 2013). Interpolated maps of velocity changes (Sibson & Barnett, 1981) for each point in time during the stick-slip cycle (Figures 2a–2d) show the spatio-temporal evolution of dc/c (Figures 2e–2h, see Supporting Information Text S3). The largest velocity variations (positive or negative, significant at 3σ) are concentrated in the slow-slipping and slow-rupturing (Figures 1c and 1d) aseismic region in the center of the WIP. The regions associated with the sticky spots and the fast slipping motion exhibit no resolvable velocity changes.

Given the frequency band of analysis and the early coda window used for the dc/c measurements, we hypothesize that the velocity change is mainly happening within the till layer at the bottom of the glacier. The early coda is dominated by Rayleigh waves, which exhibit a large sensitivity in the low velocity till layer (Figure S2) at 0.2–0.5 Hz. The strain in the ice during the slip, estimated around 10 microstrains (0.001%), is on the order of the dc/c uncertainty and is unlikely to produce the observed velocity changes (Figure S3, see Supporting Information Text S7 for a derivation of the expected velocity change in the ice due to an elastic deformation during the slip based on the sensitivity of ice shear-modulus to pressure change at pressures relevant for ice sheets (Shaw, 1986)). This estimation of the velocity-change induced by the ice deformation does not take into account potential changes in ice porosity during the cycle, that could be translated into shear-wave velocity changes. If a porosity change occurs during the stick-slip event due to the ice deformation, one can expect the change to be maximum when the deformation is maximum. However, we observe that the seismic velocity keeps decreasing even after the end of the slip (Figures 2a–2h). This indicates that the velocity changes cannot be entirely due to ice elastic deformation effects. Furthermore, according to numerical models (Lipovsky & Dunham, 2017), the associated stress in the ice in between the sticky spots is expected to result in a velocity increase. To fully resolve whether the observed velocity changes are happening only in the till layer or in the ice column, we would need to record and use higher frequencies. In this case, a denser seismic array with shorter inter-station distances would be necessary.

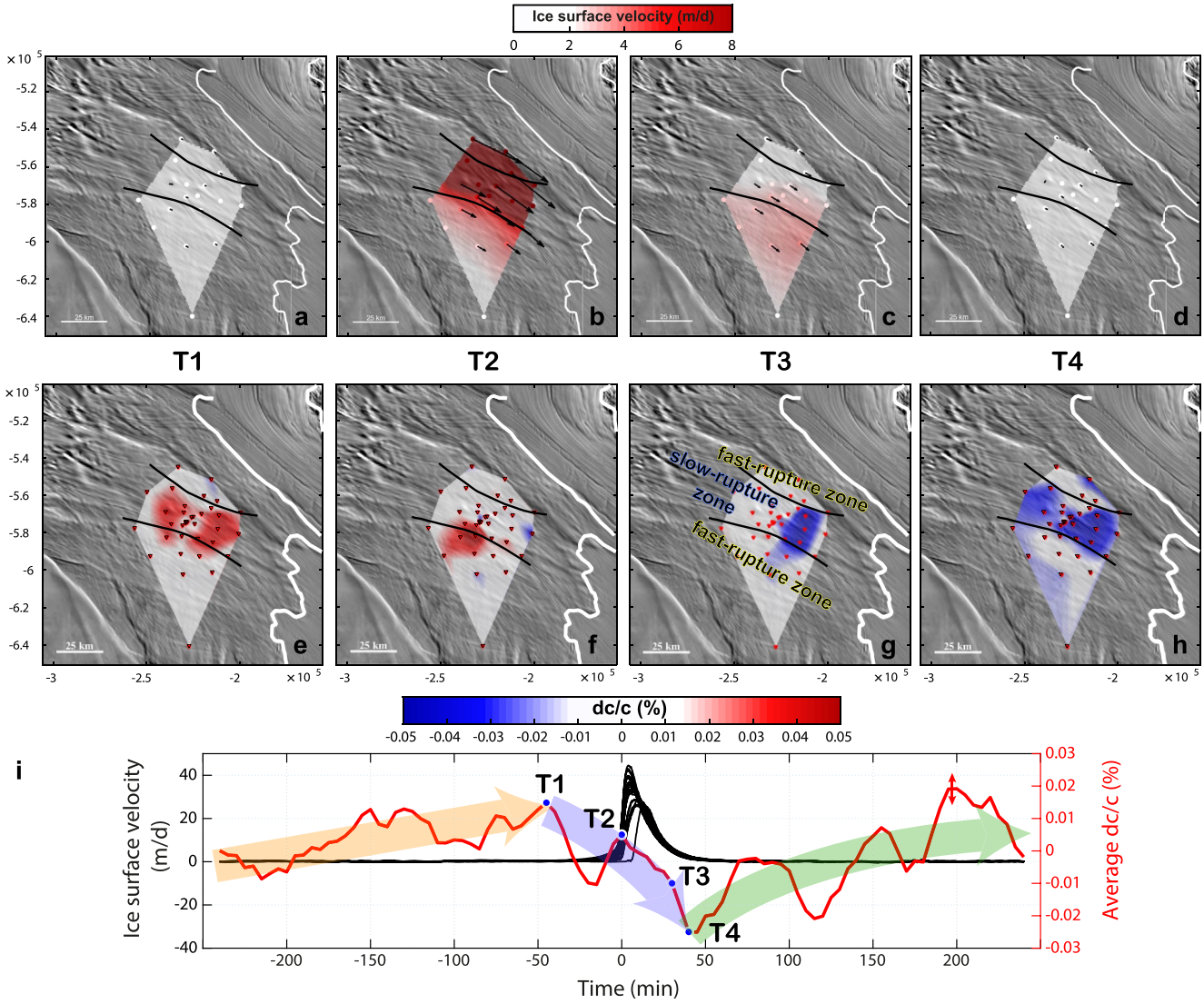

Figure 2. Relative seismic velocity variations. Maps at $T1 = 45$ min before the beginning of the slip of the average ice velocity (a) and dc/c (e), same at T2 = the onset time of the slip (b), (f), same at $T3 = 30$ min after the beginning of the slip (c), (g) and same at $T4 = 40$ min after the beginning of the slip (d), (h). Only the velocity changes larger than 3σ are shown in color, smaller changes are in white. The ice velocity colorscale is saturated at 8 m/d to highlight the rupture-front orientation and direction of propagation. The background image is a mosaic of optical images collected from MODIS (Haran et al., 2014) (a) Spatially averaged dc/c (red curve). The red double-headed arrow near 200 min represents the average 1σ error of the dc/c results. Black curves are ice surface velocities averaged over all slip events for each GPS station. The colored arrows highlight the general trends of the velocity changes.

4. Poroelastic Control of the Bed Frictional Properties

We use the theory of effective medium for fluid-saturated sediments (Dvorkin et al., 1999; Gassmann, 1951; Leeman et al., 2016; Nur et al., 1998) to relate the till shear wave velocity (Vs) to its composition, effective pressure (the difference between the pressure of the ice column and the pore pressure in the till), and porosity (see Supporting Information Text S5 for the full derivation of the poroelastic shear-wave velocity estimation). With a till layer of Vs = 350 m/s and 35% porosity (Kamb, 2001; Luthra et al., 2016), we can estimate the effective pressure in the till to be around 17 kPa (Figure 3). The local velocity drop within the till layer corresponding to the relative velocity change of −0.05% observed from the surface is estimated using Rayleigh-wave depth sensitivity kernels to be about −7.6% (see Supporting Information Text S6 and Figure S2). From this value, we can infer possible couples of effective pressure/porosity changes that explain the observed seismic velocity drop (Figure 3).

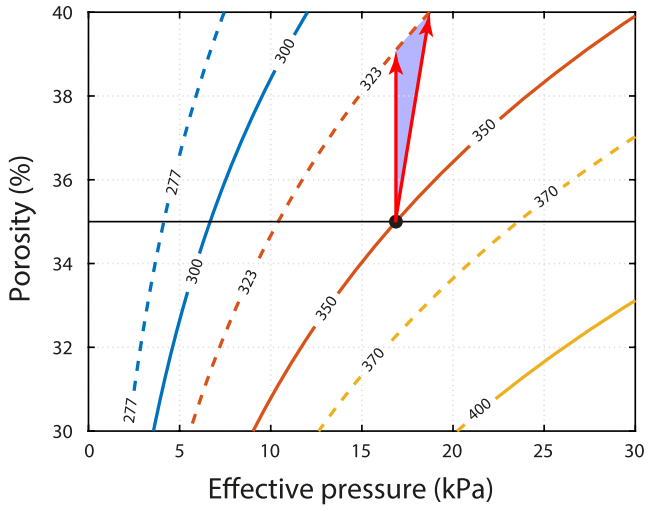

Figure 3. Poroelastic model. Colored lines with labels indicate till shear-wave velocity (m/s) as a function of effective pressure and porosity. The dashed curves represent a 7.6% decrease of velocity compared to the solid curve of the same color. Red arrows show possible trajectories of velocity reduction. The blue quadrant involves increase of both porosity and effective pressure, consistent with strengthening friction.

During a stick-slip event, the glacier starts accelerating on one sticky spot and is then slowed down in its central region where rate-strengthening friction increases the resistance to sliding at higher velocities (Lipovsky & Dunham, 2017). Acceleration then resumes at the second sticky spot. Previous seismic and geodetic observations made on the glacier showed that the sticky spots were seismogenic, whereas the central region was not (Barcheck et al., 2018; Pratt et al., 2014; Wiens et al., 2008; Winberry et al., 2009, 2011, 2013) (Figure 4), also suggesting a rate-weakening/rate-strengthening segregation of the bed properties. Several possible glaciological processes have been proposed to explain rate-strengthening behaviors (Lipovsky & Dunham, 2017): (a) Dilatant strengthening of till (Minchew & Meyer, 2020; Segall et al., 2010), (b) non-constant rate dependency of friction that could switch from rate-weakening to rate-strengthening above a certain threshold of sliding velocity (Kilgore et al., 1993; Shibazaki & Shimamoto, 2007) and (c) frictional heating due to elevated slip-rate at the bed (McCarthy et al., 2017). Dilatant strengthening of the till seems to be the phenomenon that allows for lateral variations of the friction more easily because it is controlled by the bed topography, which is the first-order source of lateral heterogeneity at the WIP. It is not clear how the two other candidates could produce such lateral heterogeneity.

Our seismic velocity change measurements demonstrate that the central part of the WIP is host to dilatant strengthening friction (Segall et al., 2010; Minchew & Meyer, 2020). This dilatancy reflects a transient increase of porosity that induces a decreased water pore pressure. This effect is amplified in areas of already high pore-pressure, in the deep

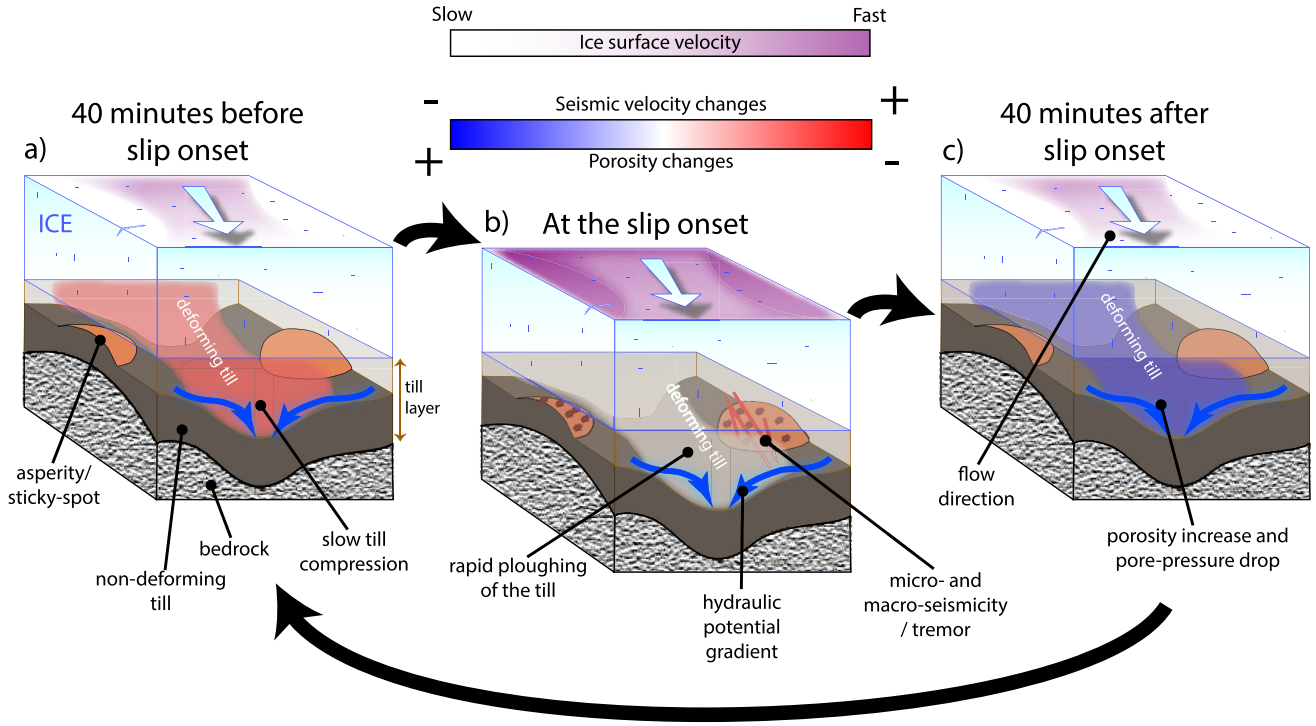

Figure 4. Conceptual model of the WIP stick-slip cycle. (a) Shear stress applied to the till by the glacier increases as the till slowly compacts under the weight of the glacier. Pore water pressures and seismic wave speeds increase as porosity decreases. (b) Shear stress reaches a threshold, causing the glacier to slip and rework the till layer. (c) Rapid slip causes the porosity of the till to increase. This dilation drives a decrease in pore water pressure, which strengthens the till and reduces seismic wave speeds.

parts of the subglacial valleys (Figure 1b). Quantitatively, by assuming a 35% porosity and a local seismic velocity reduction of −7.6%, we can infer relative porosity changes between +10% and +15%, coupled with an effective pressure increase up to 2 kPa (11% relative change, Figure 3). The exact trajectory of velocity changes in the effective pressure/porosity domain during a complete stick-slip cycle is not fully constrained by our observations, and might involve complex variations in both effective pressure and porosity. Our model, however, provides upper limits for effective pressure and porosity variations during stick-slip events.

While the proximate cause of stick-slip events on the WIP is thought to be the presence of rate-weakening friction (Winberry et al., 2009), theoretical (Lipovsky et al., 2019) and experimental (Zoet et al., 2013, 2020) considerations point to friction between entrained sediments in a dirty basal ice layer as the ultimate cause of this rate weakening friction. Sediment entrainment is generally favored at lower water pressures (Rempel, 2008). The observation of a large seismic velocity change due to shear dilatancy is therefore consistent with this theory of sediment dynamics, insofar as areas with rate weakening friction (sticky-spots) are not inferred to undergo large changes in water content.

5. Conclusion

Our study shows that the friction at the base of the WIP is controlled by a complex feedback between the bed topography, which induces spatial variability in the till layer, and the cycles of stick-slip events, which result in elevated shearing rates with accompanying dilation. This dilation, causing porosity and effective pressure increase, induces a strengthening that slows down the slip in the central part of the glacier (Figure 4). Through their influence on the stick-slip cycle, these hydromechanical processes govern the flow of WIP and illuminate the mechanics of basal slip. As a result, a complete understanding of basal slip and the processes that govern ice sheet evolution must account for the hydromechanics of subglacial till. Given the physics involved, similar phenomena should take place within tectonic fault-zones during earthquakes or tectonic slow-slip cycles (Segall et al., 2010). Being able to measure seismic velocity changes during these cycles (Rivet et al., 2014) with a similar spatial and temporal resolution could also help to unravel the physics at play during tectonic earthquakes.

Conflict of Interest

The authors declare no conflicts of interest relevant to this study.

Data Availability Statement

The facilities of IRIS Data Services, and specifically the IRIS Data Management Center, were used for access to 2C network waveforms (https://doi.org/10.7914/SN/2C_2010), related metadata, and/or derived products used in this study. IRIS Data Services are funded through the Seismological Facilities for the Advancement of Geoscience (SAGE) Award of the National Science Foundation under Cooperative Service Agreement EAR-1851048. Figures 1 and 2 have been partly made with the Antarctic mapping toolbox (Greene et al., 2017). The grounding line is from Mouginot et al. (2016) (https://doi.org/10.5067/SEVV4MR8P1ZN). Seismic data have been downloaded and instrument-corrected with ObspyDMT (Hosseini & Sigloch, 2017). The cross-correlations were computed with MSNoise (Lecocq et al., 2014).

Acknowledgments
This work was supported by the TelluS Program of CNRS/INSU, CSI Program of Université Côte d'Azur, and BQR program of Observatoire Côte d'Azur. This research was supported by the National Science Foundation under Grant No. PLR-1643761.

References

Alley, R. B. (1993). In search of ice-stream sticky spots. *Journal of Glaciology*, *39*(133), 447–454. https://doi.org/10.3189/s0022143000016336

Alley, R. B., Blankenship, D. D., Bentley, C. R., & Rooney, S. (1986). Deformation of till beneath ice stream B, West Antarctica. *Nature*, *322*(6074), 57–59. https://doi.org/10.1038/322057a0

Alley, R. B., Clark, P. U., Huybrechts, P., & Joughin, I. (2005). Ice-sheet and sea-level changes. *Science*, *310*(5747), 456–460. https://doi.org/10.1126/science.1114613

Bamber, J. L., Layberry, R. L., & Gogineni, S. (2001). A new ice thickness and bed data set for the Greenland ice sheet: 1. Measurement, data reduction, and errors. *Journal of Geophysical Research*, *106*(D24), 33773–33780. https://doi.org/10.1029/2001jd900054

Barcheck, C. G., Brodsky, E., Fulton, P., King, M., Siegfried, M., & Tulaczyk, S. (2021). Migratory earthquake precursors are dominant on an ice stream fault. *Science Advances*, *7*(6). eabd0105. https://doi.org/10.1126/sciadv.abd0105

Barcheck, C. G., Schwartz, S. Y., & Tulaczyk, S. (2020). Icequake streaks linked to potential mega-scale glacial lineations beneath an Antarctic ice stream. *Geology*, *48*(2), 99–102. https://doi.org/10.1130/g46626.1

Barcheck, C. G., Tulaczyk, S., Schwartz, S. Y., Walter, J. I., & Winberry, J.-P. (2018). Implications of basal micro-earthquakes and tremor for ice stream mechanics: Stick-slip basal sliding and till erosion. *Earth and Planetary Science Letters*, *486*, 54–60. https://doi.org/10.1016/j.epsl.2017.12.046

Bindschadler, R. A., King, M. A., Alley, R. B., Anandakrishnan, S., & Padman, L. (2003). Tidally controlled stick-slip discharge of a West Antarctic ice. *Science*, *301*(5636), 1087–1089. https://doi.org/10.1126/science.1087231

Blankenship, D. D., Bentley, C. R., Rooney, S., & Alley, R. B. (1986). Seismic measurements reveal a saturated porous layer beneath an active Antarctic ice stream. *Nature*, *322*(6074), 54–57. https://doi.org/10.1038/322054a0

Brenguier, F., Campillo, M., Takeda, T., Aoki, Y., Shapiro, N., Briand, X., et al. (2014). Mapping pressurized volcanic fluids from induced crustal seismic velocity drops. *Science*, *345*(6192), 80–82. https://doi.org/10.1126/science.1254073

Brisbourne, A. M., Smith, A. M., Vaughan, D. G., King, E. C., Davies, D., Bingham, R., et al. (2017). Bed conditions of Pine Island Glacier, West Antarctica. *Journal of Geophysical Research: Earth Surface*, *122*(1), 419–433. https://doi.org/10.1002/2016jf004033

Cornford, S. L., Seroussi, H., Asay-Davis, X. S., Gudmundsson, G. H., Arthern, R., & Borstad, C., et al. (2020). Results of the third marine ice sheet model intercomparison project (mismip+). *The Cryosphere Discussions*, *14*, 2283–2301.

Dvorkin, J., Prasad, M., Sakai, A., & Lavoie, D. (1999). Elasticity of marine sediments: Rock physics modeling. *Geophysical Research Letters*, *26*(12), 1781–1784. https://doi.org/10.1029/1999gl900332

Fretwell, P., Pritchard, H. D., Vaughan, D. G., Bamber, J. L., Barrand, N. E., Bell, R., et al. (2013). Bedmap2: Improved ice bed, surface and thickness datasets for Antarctica. *The Cryosphere*, *7*(1), 375–393. https://doi.org/10.5194/tc-7-375-2013

Gassmann, F. (1951). Elasticity of porous media. *Vierteljahrsschrder Naturforschenden Gesselschaft*, *96*, 1–23.

Golledge, N. R., Keller, E. D., Gomez, N., Naughten, K. A., Bernales, J., Trusel, L. D., & Edwards, T. L. (2019). Global environmental consequences of twenty-first-century ice-sheet melt. *Nature*, *566*(7742), 65–72. https://doi.org/10.1038/s41586-019-0889-9

Greene, C. A., Gwyther, D. E., & Blankenship, D. D. (2017). Antarctic mapping tools for matlab. *Computers & Geosciences*, *104*, 151–157. https://doi.org/10.1016/j.cageo.2016.08.003

Haran, T., Bohlander, J., Scambos, T., Painter, T., & Fahnestock, M. (2014). *MODIS Mosaic of Antarctica 2008–2009 (MOA2009) image map*. 10. https://doi.org/10.7265/N5KP8037

Hillers, G., Retailleau, L., Campillo, M., Inbal, A., Ampuero, J.-P., & Nishimura, T. (2015). In situ observations of velocity changes in response to tidal deformation from analysis of the high-frequency ambient wavefield. *Journal of Geophysical Research: Solid Earth*, *120*(1), 210–225. https://doi.org/10.1002/2014jb011318

Hobiger, M., Wegler, U., Shiomi, K., & Nakahara, H. (2012). Coseismic and postseismic elastic wave velocity variations caused by the 2008 Iwate-Miyagi Nairiku earthquake, Japan. *Journal of Geophysical Research*, *117*(B9). https://doi.org/10.1029/2012jb009402

Hosseini, K., & Sigloch, K. (2017). ObspyDMT: A Python toolbox for retrieving and processing large seismological data sets. *Solid Earth*, *8*(5), 1047–1070. https://doi.org/10.5194/se-8-1047-2017

Iverson, N. R., Cohen, D., Hooyer, T. S., Fischer, U. H., Jackson, M., Moore, P. L., & Kohler, J. (2003). Effects of basal debris on glacier flow. *Science*, *301*(5629), 81–84. https://doi.org/10.1126/science.1083086

Jones, R. (1975). An approximate expression for the fundamental frequency of vibration of elastic plates. *Journal of Sound and Vibration*, *38*(4), 503–504. https://doi.org/10.1016/s0022-460x(75)80139-8

Joughin, I., Bindschadler, R., King, M., Voigt, D., Alley, R. B., Anandakrishnan, S., et al. (2005). Continued deceleration of Whillans ice stream, West Antarctica. *Geophysical Research Letters*, *32*(22). https://doi.org/10.1029/2005gl024319

Kamb, B. (2001). Basal zone of the west antarctic ice streams and its role in lubrication of their rapid motion. *The West Antarctic Ice Sheet: Behavior And Environment*, *77*, 157–199. https://doi.org/10.1029/AR077p0157

Kilgore, B. D., Blanpied, M. L., & Dieterich, J. H. (1993). Velocity dependent friction of granite over a wide range of conditions. *Geophysical Research Letters*, *20*(10), 903–906. https://doi.org/10.1029/93gl00368

Lecocq, T., Caudron, C., & Brenguier, F. (2014). MSNoise, a python package for monitoring seismic velocity changes using ambient seismic noise. *Seismological Research Letters*, *85*(3), 715–726. https://doi.org/10.1785/0220130073

Leeman, J., Valdez, R., Alley, R., Anandakrishnan, S., & Saffer, D. (2016). Mechanical and hydrologic properties of Whillans Ice Stream till: Implications for basal strength and stick-slip failure. *Journal of Geophysical Research: Earth Surface*, *121*(7), 1295–1309. https://doi.org/10.1002/2016jf003863

Lipovsky, B. P., & Dunham, E. (2016). Tremor during ice-stream stick slip. *The Cryosphere*, *10*(1), 385–399. https://doi.org/10.5194/tc-10-385-2016

Lipovsky, B. P., & Dunham, E. M. (2017). Slow-slip events on the whillans ice plain, antarctica, described using rate-and-state friction as an ice stream sliding law. *Journal of Geophysical Research: Earth Surface*, *122*(4), 973–1003. https://doi.org/10.1002/2016jf004183

Lipovsky, B. P., Meyer, C. R., Zoet, L. K., McCarthy, C., Hansen, D. D., Rempel, A. W., & Gimbert, F. (2019). Glacier sliding, seismicity and sediment entrainment. *Annals of Glaciology*, *60*(79), 182–192. https://doi.org/10.1017/aog.2019.24

Luthra, T., Anandakrishnan, S., Winberry, J.-P., Alley, R. B., & Holschuh, N. (2016). Basal characteristics of the main sticky spot on the ice plain of Whillans Ice Stream, Antarctica. *Earth and Planetary Science Letters*, *440*, 12–19. https://doi.org/10.1016/j.epsl.2016.01.035

McCarthy, C., Savage, H., & Nettles, M. (2017). Temperature dependence of ice-on-rock friction at realistic glacier conditions. *Philosophical Transactions of the Royal Society A: Mathematical, Physical & Engineering Sciences*, *375*, 20150348. https://doi.org/10.1098/rsta.2015.0348

Meyer, C. R., Downey, A. S., & Rempel, A. W. (2018). Freeze-on limits bed strength beneath sliding glaciers. *Nature Communications*, *9*(1), 1–6. https://doi.org/10.1038/s41467-018-05716-1

Minchew, B., & Meyer, C. R. (2020). Dilation of subglacial sediment governs incipient surge motion in glaciers with deformable beds. *Proceedings of the Royal Society A*, *476*(2238). 20200033. https://doi.org/10.1098/rspa.2020.0033

Minchew, B., Simons, M., Riel, B., & Milillo, P. (2017). Tidally induced variations in vertical and horizontal motion on rutford ice stream, west antarctica, inferred from remotely sensed observations. *Journal of Geophysical Research: Earth Surface*, *122*(1), 167–190. https://doi.org/10.1002/2016jf003971

Mordret, A., Mikesell, T. D., Harig, C., Lipovsky, B. P., & Prieto, G. A. (2016). Monitoring southwest Greenland's ice sheet melt with ambient seismic noise. *Science advances*, *2*(5). e1501538. https://doi.org/10.1126/sciadv.1501538

Moreau, L., Stehly, L., Boué, P., Lu, Y., Larose, E., & Campillo, M. (2017). Improving ambient noise correlation functions with an SVD-based Wiener filter. *Geophysical Journal International*, *211*(1), 418–426. https://doi.org/10.1093/gji/ggx306

Mouginot, J., Scheuchl, B., & Rignot, E. (2016). Measures antarctic boundaries for ipy 2007–2009 from satellite radar, version 1. NASA National Snow and Ice Data. Center Distributed Active Archive Center, USA, Data accessed: 2021-05-07. https://doi.org/10.5067/SEVV4MR8P1ZN

Nicholls, R. J., & Cazenave, A. (2010). Sea-level rise and its impact on coastal zones. *Science*, *328*(5985), 1517–1520. https://doi.org/10.1126/science.1185782

Nur, A., Mavko, G., Dvorkin, J., & Galmudi, D. (1998). Critical porosity: A key to relating physical properties to porosity in rocks. *The Leading Edge*, *17*(3), 357–362. https://doi.org/10.1190/1.1437977

Obermann, A., Planes, T., Larose, E., Sens-Schönfelder, C., & Campillo, M. (2013). Depth sensitivity of seismic coda waves to velocity perturbations in an elastic heterogeneous medium. *Geophysical Journal International*, *194*(1), 372–382. https://doi.org/10.1093/gji/ggt043

Oppenheimer, M. (1998). Global warming and the stability of the West Antarctic Ice Sheet. *Nature*, *393*(6683), 325–332. https://doi.org/10.1038/30661

Pachauri, R. K., Allen, M. R., Barros, V. R., Broome, J., Cramer, W., Christ, R., et al. (2014). Ipcc.Climate change 2014: Synthesis report. Contribution of working groups I, II and III to the fifth assessment report of the intergovernmental panel on climate change

Pratt, M. J., Winberry, J.-P., Wiens, D. A., Anandakrishnan, S., & Alley, R. B. (2014). Seismic and geodetic evidence for grounding-line control of Whillans Ice Stream stick-slip events. *Journal of Geophysical Research: Earth Surface*, *119*(2), 333–348. https://doi.org/10.1002/2013jf002842

Rempel, A. (2008). A theory for ice-till interactions and sediment entrainment beneath glaciers. *Journal of Geophysical Research*, *113*(F1). https://doi.org/10.1029/2007jf000870

Rivet, D., Campillo, M., Radiguet, M., Zigone, D., Cruz-Atienza, V., Shapiro, N. M., et al. (2014). Seismic velocity changes, strain rate and non-volcanic tremors during the 2009–2010 slow slip event in Guerrero, Mexico. *Geophysical Journal International*, *196*(1), 447–460. https://doi.org/10.1093/gji/ggt374

Robel, A. A., Tsai, V. C., Minchew, B., & Simons, M. (2017). Tidal modulation of ice shelf buttressing stresses. *Annals of Glaciology*, *58*(74), 12–20. https://doi.org/10.1017/aog.2017.22

Schoof, C. (2005). The effect of cavitation on glacier sliding. *Proceedings of the Royal Society A*, *461*, 609–627. https://doi.org/10.1098/rspa.2004.1350

Segall, P., Rubin, A. M., Bradley, A. M., & Rice, J. R. (2010). Dilatant strengthening as a mechanism for slow slip events. *Journal of Geophysical Research*, *115*(B12). https://doi.org/10.1029/2010jb007449

Shaw, G. H. (1986). Elastic properties and equation of state of high pressure ice. *The Journal of Chemical Physics*, *84*(10), 5862–5868. https://doi.org/10.1063/1.449897

Shibazaki, B., & Shimamoto, T. (2007). Modeling of short-interval silent slip events in deeper subduction interfaces considering the frictional properties at the unstable-stable transition regime. *Geophysical Journal International*, *171*(1), 191–205. https://doi.org/10.1111/j.1365-246x.2007.03434.x

Sibson, R., & Barnett, V. (1981). Interpreting multivariate data. *A brief description of natural neighbor interpolation*, 21–36.

Siegfried, M. R., & Fricker, H. A. (2018). Thirteen years of subglacial lake activity in Antarctica from multi-mission satellite altimetry. *Annals of Glaciology*, *59*, 42–55. https://doi.org/10.1017/aog.2017.36

Silver, P. G., Daley, T. M., Niu, F., & Majer, E. L. (2007). Active source monitoring of cross-well seismic travel time for stress-induced changes. *Bulletin of the Seismological Society of America*, *97*(1B), 281–293. https://doi.org/10.1785/0120060120

Stokes, C. R., Clark, C. D., Lian, O. B., & Tulaczyk, S. (2007). Ice stream sticky spots: A review of their identification and influence beneath contemporary and palaeo-ice streams. *Earth-Science Reviews*, *81*(3–4), 217–249. https://doi.org/10.1016/j.earscirev.2007.01.002

Tulaczyk, S., Kamb, W. B., & Engelhardt, H. F. (2000). Basal mechanics of ice stream B, West Antarctica: 1. Till mechanics. *Journal of Geophysical Research*, *105*(B1), 463–481. https://doi.org/10.1029/1999jb900329

Weertman, J. (1964). The theory of glacier sliding. *Journal of Glaciology*, *5*(39), 287–303. https://doi.org/10.3189/s0022143000029038

Wiens, D. A., Anandakrishnan, S., Winberry, J.-P., & King, M. A. (2008). Simultaneous teleseismic and geodetic observations of the stick–slip motion of an Antarctic ice stream. *Nature*, *453*(7196), 770–774. https://doi.org/10.1038/nature06990

Winberry, J.-P., Anandakrishnan, S., Alley, R. B., Bindschadler, R. A., & King, M. A. (2009). Basal mechanics of ice streams: Insights from the stick-slip motion of Whillans Ice Stream, West Antarctica. *Journal of Geophysical Research*, *114*(F1). https://doi.org/10.1029/2008jf001035

Winberry, J.-P., Anandakrishnan, S., Alley, R. B., Wiens, D. A., & Pratt, M. J. (2014). Tidal pacing, skipped slips and the slowdown of Whillans Ice Stream, Antarctica. *Journal of Glaciology*, *60*(222), 795–807. https://doi.org/10.3189/2014jog14j038

Winberry, J.-P., Anandakrishnan, S., Wiens, D. A., Alley, R. B., & Christianson, K. (2011). Dynamics of stick–slip motion, Whillans Ice Stream, Antarctica. *Earth and Planetary Science Letters*, *305*(3–4), 283–289. https://doi.org/10.1016/j.epsl.2011.02.052

Winberry, J.-P., Anandakrishnan, S., Wiens, D., & Alley, R. (2013). Nucleation and seismic tremor associated with the glacial earthquakes of Whillans Ice Stream, Antarctica. *Geophysical Research Letters*, *40*, 312–315. https://doi.org/10.1002/grl.50130

Wu, P.-K., Matsushima, K., & Tatsuoka, F. (2008). Effects of specimen size and some other factors on the strength and deformation of granular soil in direct shear tests. *Geotechnical Testing Journal*, *31*(1), 45–64

Zoet, L. K., Carpenter, B., Scuderi, M., Alley, R. B., Anandakrishnan, S., Marone, C., & Jackson, M. (2013). The effects of entrained debris on the basal sliding stability of a glacier. *Journal of Geophysical Research: Earth Surface*, *118*(2), 656–666. https://doi.org/10.1002/jgrf.20052

Zoet, L. K., Ikari, M., Alley, R., Marone, C., Anandakrishnan, S., Carpenter, B., & Scuderi, M. (2020). Application of constitutive friction laws to glacier seismicity. *Geophysical Research Letters*, *47*(21). e2020GL088964. https://doi.org/10.1029/2020gl088964

Zoet, L. K., & Iverson, N. R. (2020). A slip law for glaciers on deformable beds. *Science*, *368*(6486), 76–78. https://doi.org/10.1126/science.aaz1183